

EFFECTS OF THE RATE OF CYCLIC LOADING ON THE INELASTIC BEHAVIOR OF REINFORCED CONCRETE COLUMNS

T. Arakawa (I)

Y. Arai (II)

Presenting Author : T. Arakawa

SUMMARY

Eighteen half-size columns were tested to study the effects of cyclic loading rate and behavior on the inelastic deformation capacity of reinforced concrete columns. The failure modes and load-carrying capacities of the columns were found virtually not to be affected by the loading rate, levels of axial load, concrete strengths, shear span ratios and longitudinal tension steel ratios. However, the ductility factors as one of inelastic deformation capacity were found specifically influenced by these factors. These ductility factors obtained from the tests were evaluated similarly with the analytical values proposed herein.

INTRODUCTION

It is an important subject for the earthquake resistant design of reinforced concrete structures to estimate adequately the inelastic deformation capacity of the members under cyclic loading. Experimental investigations on the behavior of structural members subjected to slow cyclic loading rate have been carried out by many researchers. No general rules, however, have been established yet to evaluate quantitatively the differences between slow and high rates of cyclic loading.

The first objective of this investigation is to experimentally determine the effect of loading rate on the cyclic behavior of reinforced concrete columns. The second objective is to compare the performance of the columns in this test with that of the past test data and to obtain a means for evaluating the inelastic deformation capacity of columns quantitatively.

EXPERIMENTAL PROGRAM

Test Specimens—The details of 18 specimens selected for this experiment are shown in Fig.1 and Table 1. The cross section of a column is a 25 cm square. The variables of columns included the shear span ratio M/QD , concrete strength F_c , level of axial load N (compressive stress $\sigma_0 = N/bD$), longitudinal tension steel ratio P_t and shear reinforcement ratio $P_w (= 0.30 \sim 1.50\%)$. These specimens were divided into the following two series:

Series I: Ten columns of No.201~210 designed under the same condition were prepared to study the effects of loading rate.

Series II: Eight columns of No.211~218 were prepared to study the effects of F_c (No.212, 213, 214), P_t (No.215, 216, 217), M/QD (No.212, 217, 218) and σ_0 (No.204, 211, 212) on the cyclic loading behavior.

The shear reinforcement ratios in Series I and II were decided to prevent the occurrence of shear failure prior to the flexural failure. The values of P_w were obtained from the following relationship with references to the existing test results [1, 2, 3]:

(I) Prof. of Structural Engineering, Muroran Inst. of Tech., Hokkaido.

(II) Asst. Prof. of Structural Eng., Muroran Inst. of Tech., Hokkaido.

$$cQ_{BU} = 0.82 cQ_{su} \dots\dots\dots(1)$$

in which, cQ_{BU} = shear at ultimate flexural strength; cQ_{su} = shear at ultimate shear strength [7] (see the footnote of Table 4).

Properties of Materials and Fabrication of Test Specimens—The physical properties of materials are summarized in Table 2. All the specimens were horizontally cast in metal forms. Two days after casting the forms were removed. All the columns and test cylinders (10 cm ϕ x 20 cm) were cured in the same condition with plastic sheets covering until the 70% of designed concrete strength was attained. The tests were carried out at about four weeks after casting.

Loading Apparatus—As shown in Fig.2, the specimen was horizontally supported at two points (corresponding to the points of A and B in Fig.1) in the steel testing frame which was fixed vertically on the test floor. The two imaginary inflection points of the beams were connected with the steel yolk which allowed rotation through the needle bearing. The horizontal load was applied by an oil pressure servo-pulse type actuator (± 30 ton of capacity and ± 10 cm of stroke) at the free ends of the beam. During the test a 50 ton oil jack attached to the column gave a fixed axial load through four external bars.

Loading Program—As illustrated in Fig.3, the cyclic loading pattern which is controlled by the horizontal deflection was used for these tests. For all the columns, the horizontal deflections were increased progressively from beginning to end of the loading. These loading programs are listed in Table 3.

In Series I, the column No.201 was supposed to be the representative column which was tested under the slow displacement rate. This column was tested with the frequency $f_r = 0.05$ Hz, the increasing pitch of displacement amplitude $p = 0.40$ mm/cycle and the displacement rate $v = 0.02$ mm/sec. Other 9 columns (No. 202~210) were tested to compare the differences of f_r , p and v .

In Series II, all the columns (No.211~218) were tested with $f_r = 1.0$ Hz and $p = 0.2$ mm/cycle ($v = 0.2$ mm/sec).

Measurements—Load cells incorporated in the apparatus were used to measure the applied horizontal load, axial load and shear force of beams. The horizontal deflections at the top and bottom of a column were measured with linear differential transformers attached to the gauge holder fixed in the beam-to-column joints on one side of the column. One of the measured deflections was used to control the actuator as the displacement feedback signals during the tests. The strain in the longitudinal steel and transverse shear reinforcement at the several locations marked O in Fig.1 were measured continuously throughout the tests. All the measured values were recorded on a tape recorder and were processed by a computer.

TEST RESULTS AND DISCUSSION

Cracks and Failure Modes—The flexural and shear cracking regions for the columns showed a tendency to become a little wider with the decreases of f_r and F_c , and with the increases of P_t and σ_0 . Concerning the failure modes, all the hinging zone of a column after the longitudinal tension steel had yielded. However, no evident differences were observed for the variables of p , v , M/QD , F_c , P_t and σ_0 .

Stiffness at Yielding—The ratios of the measured stiffness at yielding to the

computed values by the AIJ Code are within the limits of 0.73~1.14 (average 0.98) and all the test results are found to be in better agreement with the computed values.

Yield Loads and Load-Carrying Capacities—As shown in Figs.4(a)~(d), the measured horizontal shear forces tQ are higher than the computed values cQ . The load ratios of tQ/cQ are within the limits of 1.00~1.16 (average 1.11) for the yield loads and 1.04~1.20 (average 1.14) for the maximum loads. However, these ratios are almost not affected by the variations of v and axial load factor η_0 ($=\sigma_0/F_c$) as shown in Figs.4(a) and (b). On the other hand, these ratios showed a tendency to become smaller with increases of M/QD and P_t as shown in Figs.4 (c) and (d).

Load-Deflection Envelope Curves—The maximum loads reached about 1.05 times as much as the measured yield loads as shown in Fig.5. The load-carrying capacities after maximum loads decreased gradually with increasing the cyclic deflections. This deteriorations in load-carrying capacities may be caused by the combinations of the concrete fatigue, loss of bond in main reinforcing steel and splitting of concrete cover at the hinging zone. Consequently, the measured limits of displacement angle Rou ($=\delta_{ou}/h_0$, δ_{ou} is measured deflection shown in Fig.6) marked x in Fig.5 showed a tendency to become a little larger with decreasing p and P_t , and with increasing σ_0 .

Ductility Factor—The two measured displacement ductility factors are defined as shown in Fig.6. One is a ductility factor $t\mu$ at maximum load and the other is a limit of ductility factor $t\mu_{ou}$ at the limit of displacement.

In the tests of Series I, the values of $t\mu$ are not significantly affected by the increases of p and f_r as shown in Figs.7(a) and (b). However, the values of $t\mu_{ou}$ indicated lower values with the decrease of p , when f_r is constant.

On the other hand, when p is constant, the values of $t\mu_{ou}$ are almost kept at constant values regardless of the variations of v .

In the tests of Series II, the values of $t\mu$ and $t\mu_{ou}$ are not affected significantly by the values of M/QD and P_t as shown in Figs.8(a) and (b). However, these ductility factors are decreased hyperbolically with increasing η_0 as shown in Fig.8(c). In this case, if the values of Δ ($=p/t\delta_y$) are within the limits of 0.05~0.15 (average 0.10), the limit of ductility factors $t\mu_{ou}$ can be expressed by the Eq.2 as well as the test results in Refs.2 and 4.

$$t\mu_{ou} = 1/(\eta_0 + 0.1) \dots\dots\dots (2)$$

Empirical Formulae—Fig.9 shows the relationship between $t\mu_{ou}$ and Δ by using the data of a total 18 specimens (all $M/QD=1.5$), 10 of which are described in this paper and 8 in Ref.1. Now, assuming that the values of $t\mu_{ou}$ can be expressed as $t\mu_{ou} = A\Delta^B + 1.0$, and computing the values of A and B by the regression analysis, the following empirical formula can be obtained:

$$t\mu_{ou} = 3.16 \Delta^{0.33} + 1.0 \dots\dots\dots (3)$$

The values of $t\mu_{ou}$ are evaluated variously by the differences of η_0 and Δ as shown in Eqs.2 and 3, even if the columns are designed under the same condition. Therefore, in order to convert the $t\mu_{ou}$ of columns tested with $\Delta \neq 0.1$ into that of columns with $\Delta=0.1$, it is necessary to establish the modifying coefficient (Y_{ou}) as corrections can be done easily. Since the value of $t\mu_{ou}$ is equal to 2.478 when $\Delta=0.1$, the value of Y_{ou} can be expressed as:

$$Y_{ou} = 2.478 / (3.16 \Delta^{0.33} + 1.0) \approx 1 / (1.28 \Delta^{0.33} + 0.4) \dots\dots\dots (4)$$

By using the Eqs.2 and 4, the following general expression on the limit of ductility factor for the columns tested with the arbitrary Δ is given:

$$\mu_{ou} = 1/(\eta_0 + 0.1) \gamma_{ou} = (1.28 \Delta^{0.33} + 0.4)/(\eta_0 + 0.1) \dots\dots\dots(5)$$

Comparison of Test Results and Calculated Values on μ_{ou} —Fig.10 shows the relationship between the calculated values based on Eq.5 and measured values of μ_{ou} obtained from the test data of a total 68 specimens (18 of them are reported herein and 50 are obtained from Refs.1~6). The scope of these experimental variables are summarized in Table 5.

As shown in Fig.10, 90% of the total data are within the range of $\pm 20\%$ of computed values. The average ratio of measured values to computed values was 0.998 and the standard deviation was 0.129. Consequently, if the strength ratio $K = 0.73 \sim 0.86$ (average 0.81) was used for the design of the shear reinforcement, it can be concluded that the Eq.5 predicts reasonable results.

Assumption for the Analysis—The following three assumptions are made:

(1) The envelope curves obtained from the peak loads and peak deflections in each cycle of the loading history can be indicated by the bi-linear type as shown in Fig.11(a).

(2) The main factor which is affected by the cyclic loading is the increasing displacement ratio Δ ($= p/t\delta y$) and the load-carrying capacity ratio of Q/Q_y is reached 1 at the n th cycle (n =number of cycles at the $Q/Q_y = 1$ after yield loads). In this case the value of μ_{ou} is expressed as:

$$\mu_{ou} = n \cdot \Delta + 1 \dots\dots\dots(6)$$

(3) The cyclic sequence of bi-linear model is shown in Fig.11(b). In this figure, since $\Delta A17 = \Delta A06$ and $\Delta B03 = \Delta B4$, the area of $\square O189$ equals to $\square 6789$. And then, the value of μ_{ou} can be obtained from the accumulation of loop area in each cycle.

Analytical Results—The accumulation of the nondimensional area A_{cy} , from the first yielding deflection to the displacement limit at n th cycle, i.e., energy absorbed, is obtained from the following equation [see Fig.11(a)]:

$$\Sigma A_{cy} = \square OA11' + \square OA22' + \dots\dots\dots + \square OAnn' = n(n+1) \Delta / 2 \dots\dots\dots(7)$$

Therefore, the accumulated displacement energy ΣS_{cy} (correspond to the accumulation of loop area in each cycle) is expressed as [Fig.11(b)]:

$$\Sigma S_{cy} = 2 \delta y Q_y \Sigma A_{cy} = \delta y Q_y n(n+1) \Delta \dots\dots\dots(8)$$

Substituting the solution of Eq.8 for n into Eq.6, Eq.6 is rearranged as follows:

$$\mu_{ou} = \left(\sqrt{\frac{\Sigma S_{cy}}{Q_y \delta y \Delta}} + \frac{1}{4} - \frac{1}{2} \right) \Delta + 1.0 \dots\dots\dots(9)$$

The value of ΣS_{cy} in Eq.9 is changed by the factors of Δ , M/QD , P_t and σ_0 . According to the statistical analysis of the data of 68 specimens, the value of ΣS_{cy} is given by the following empirical formula:

$$\Sigma S_{cy} = (A - B)/\Delta + (50 - A) \dots\dots\dots(10)$$

in which, the coefficients A and B are obtained from the following formulae:

$$A = 1.13 (P_t - 0.17) (M/QD + 0.54) (84.7 - \sigma_0)$$

$$B = 0.064 (P_t - 0.041) (6.0 - M/QD) (101 - \sigma_0)$$

Fig.12 shows the comparison of the measured μ_{ou} and computed values of

μ_{ou} obtained from Eqs. 9 and 10. It should be noted that the values obtained from Eqs. 9 and 10 predicted similar results to Eq. 5 (Fig. 10). This means that the value of ΣS_{cy} obtained from Eq. 10 is almost similar to the value obtained from the relation of Eq. 4 = Eq. 9.

CONCLUSIONS

Based on these tests, the following conclusions can be made:

(1) The failure modes, yield strengths and load-carrying capacities of the columns are virtually not affected by the variations of v , f_r , p , F_c , P_t , M/QD and σ_0 within the limits of this investigation.

(2) The limit of ductility factors of the columns (μ_{ou}), defined as an index to evaluate the inelastic deformation capacity, are significantly affected by the increasing displacement ratio Δ and the axial load factor η_0 . In this case, the value of μ_{ou} can be obtained from the empirical formula Eq. 5, if f_r is smaller than 2 Hz and the load-carrying capacity ratio K is within the range of 0.73~0.86 (average 0.81).

(3) In order to convert the value μ_{ou} of the columns tested with $\Delta \neq 0.1$ into that of the columns with $\Delta = 0.1$, it is effective to use the modifying coefficient Y_{ou} given by Eq. 4.

(4) The calculated values obtained from Eq. 5 can be evaluated similarly with the analytical values of Eq. 9 which is the formula of accumulated displacement energy based on the bi-linear model.

ACKNOWLEDGMENT

This experimental research was supported by the Grant-in-Aid for Scientific Research, the Ministry of Education, Science and Culture of Japan in 1982. The authors wish to express their gratitude to Assistant M. Mizoguchi, Technician T. Maruyama, Graduate Students K. Egashira, S. Ohkubo and K. Honma for their assistance in the experiment.

REFERENCES

- 1) ARAKAWA, T., et al., "Effects of the Rate of Cyclic Loading on the Load-Carrying Capacity and Inelastic Behavior of Reinforced Concrete Columns," Trans. of the Japan Concrete Institute Vol. 4, 1982, pp. 485—492.
- 2) ARAKAWA, T., et al., "Evaluation of Deformational Behavior of Reinforced Concrete Columns under Cyclic Loading," Trans. of the JCI Vol. 3, 1981, pp. 391—398.
- 3) ARAKAWA, T., Y. ARAI and Y. FUJITA, "Effectiveness of Shear Reinforcement on the Deformation Behavior of Reinforced Concrete Columns under Cyclic Loadings," Trans. of the JCI Vol. 2, 1980, pp. 439—446.
- 4) ARAKAWA, T., et al., "Effect of Loading History on the Deformational Behavior of Reinforced Concrete Columns (Part 5)," Reports of the Hokkaido Branch of the Architectural Inst. of Japan, No. 55, 1982, pp. 91—94 (in Japanese).
- 5) ARAKAWA, T., et al., "Effect of Loading History on the Deformational Behavior of Reinforced Concrete Columns (Part 1: Test Results)," Proceedings of Annual Meeting of AIJ, 1980, pp. 1741—1742 (in Japanese).
- 6) ARAKAWA, T. and N. TSUNODA, "Hysteretic Behavior of Reinforced Concrete Columns Subjected to Dynamic Lateral Loads," Proceedings of Annual Meeting of AIJ, 1979, pp. 1295—1296 (in Japanese).
- 7) SHIBATA, T., "Ultimate Strength Equations of Reinforced Concrete Members at Brittle Failure," Concrete Journal of JCI, Vol. 18, No. 1, 1980 (in Japanese).

Table 1 Kinds of Specimen

Column No.	M. QD	F _c kg/cm ²	σ ₀ kg/cm ²	Reinforcement		
				Pt (%)	Shear reinf. No. Size · @	Pw (%)
201~210	1.5	210	70	0.342	4-6φ #33	1.154
211	1.5	210	25	0.342	2-6φ #58	0.328
212	1.5	210	50	0.342	4-6φ #43	0.886
213	1.5	270	50	0.342	4-6φ #49	0.777
214	1.5	360	50	0.342	3-6φ #54	0.529
215	2.0	210	50	0.607	4-6φ #40	0.952
216	2.0	210	50	0.813	6-6φ #38	1.503
217	2.0	210	50	0.342	3-6φ #59	0.484
218	2.5	210	50	0.342	2-6φ #63	0.302

Table 2 Material Properties

	Size	Sectional Area (cm ²)	Yield Point σ _y (kg/cm ²)	Elastic Modu. Es (x10 ⁶ kg/cm ²)
Longitudinal Steel	D19	(2.870)	3950	1.81
	D13	(1.267)	3920	1.83
	D10	(0.713)	4020	1.80
	Stirrup 6φ	0.238	3110	1.98
Concrete	Sand < 5mm, f.m. = 2.72, Specific gravity = 2.65			
	Gravel < 25mm, f.m. = 7.30, Specif. gravity = 2.63			
	for F _c = 210, w/c = 0.68, Mix. prop. = 1:3.92:3.90			
	for F _c = 270, w/c = 0.60, Mix. prop. = 1:3.41:3.93			
	for F _c = 360, w/c = 0.49, Mix. prop. = 1:2.54:3.14			

Table 3 Loading Program

Increasing Pitch of Def. p	Frequency fr			
	2.0 Hz	1.0 Hz	0.5 Hz	0.05 Hz
0.80 mm/cycle			v = 0.40 No. 209	
0.40 mm/cycle		v = 0.40 No. 203	v = 0.20 No. 202	v = 0.02 No. 201
0.20 mm/cycle	v = 0.40 No. 206	v = 0.20 No. 204 211~218	v = 0.10 No. 210	
0.10 mm/cycle	v = 0.20 No. 207	v = 0.10 No. 205		
0.05 mm/cycle	v = 0.10 No. 208			

Table 5 Scope of Test Data

b x D	25 cm x 25 cm
K = cQ _{BU} /cQ _{SU}	0.728 ~ 0.855 (mean 0.81)
M/QD	1.5 ~ 2.5
F _c	198 ~ 345 (kg/cm ²)
σ ₀ = N/bD	25 ~ 70 (kg/cm ²)
Pt	0.34 ~ 0.81 %
Pw	0.10 ~ 1.50 %
Δ	0.014 ~ 1.164

Table 4 Test Results

Column No.	F _c kg/cm ²	At Yielding Load					At Maximum Load					At Limit				Failure Mode
		Cycle	n ₀	tQ _y (ton)	tδ _y (mm)		Cycle	n ₀	tQ _u (ton)	tδ _u (mm)	tμ _u	Cycle	n ₀	tδ _{ou} (mm)	tμ _{ou}	
201	223	12.0	0.305	15.98	4.75		17	0.306	16.66	6.90	1.45	26.5	0.306	10.95	2.31	49 F C
202	198	12.0	0.328	15.57	4.58		17	0.329	16.38	6.94	1.52	27.5	0.330	11.46	2.50	39 F C
203	208	12.5	0.336	15.98	4.59		17	0.337	16.91	6.76	1.47	27.5	0.339	11.28	2.46	37 F C
204	215	27.0	0.326	16.19	4.47		35	0.327	17.06	6.39	1.43	53.5	0.329	10.10	2.26	79 F C
205	233	49.0	0.301	16.11	4.91		69	0.302	16.85	6.91	1.41	89.5	0.302	9.28	1.89	116 F C
206	230	24.5	0.305	16.42	4.65		35	0.306	17.16	7.09	1.52	47.5	0.307	9.65	2.08	59 F C
207	216	40.5	0.322	15.33	4.61		50	0.322	15.98	5.96	1.29	75	0.323	9.06	1.97	97 F C
208	211	92.5	0.332	15.28	4.65		124	0.332	15.87	6.42	1.38	158	0.333	8.63	1.86	213 F C
209	205	6.0	0.344	16.23	4.41		9	0.345	17.00	6.77	1.54	14.5	0.347	11.05	2.51	26 F C
210	205	26.0	0.343	15.76	5.09		32	0.343	16.26	6.58	1.29	44.5	0.344	9.10	1.79	70 F C
211	204	21.0	0.127	10.35	4.10		56	0.135	11.46	11.38	2.78	90	0.137	18.31	4.47	98 F C Bu
212	215	24.0	0.237	13.86	4.76		38	0.239	14.55	7.80	1.64	61	0.241	12.73	2.67	82 F C
213	275	24.0	0.184	14.57	4.76		43	0.187	15.22	9.13	1.92	61	0.189	12.76	2.68	77 F C
214	345	20.5	0.149	14.79	4.00		46	0.152	15.89	9.63	2.41	70	0.154	14.77	3.69	81 F C
215	222	40.5	0.228	12.29	8.19		55	0.229	12.90	11.28	1.38	77	0.230	15.89	1.94	102 F C
216	210	44.0	0.248	13.75	8.59		64	0.249	14.70	13.11	1.53	96	0.250	19.55	2.28	101 F C
217	224	28.0	0.228	10.21	5.71		45	0.230	10.74	9.44	1.65	71.5	0.232	14.92	2.61	97 F C
[Note] 218	226	37.5	0.224	7.88	7.36		60	0.226	8.32	12.26	1.67	90	0.227	18.96	2.58	123 F C

$\eta_0 = N/bD F_c$ = axial load factor, N = axial load, bD = sectional area of column;
 tQ_y, tδ_y = measured shear and deflection at yielding of longitudinal steel (average value of positive and negative);
 tQ_u, tδ_u = measured shear and deflection at ultimate maximum load (average value);
 tδ_u, tδ_{ou} = measured deflection defined in Fig.6;
 tμ_u = tδ_u/tδ_y = measured ductility factor at maximum load;
 tμ_{ou} = tδ_{ou}/tδ_y = measured limit of ductility factor; Failure Mode: F = yielding of longitudinal steel, C = crushing of concrete, B = buckling of steel;
 $cQ_y = \{g_1 \alpha t \sigma_y D + 0.5 \eta_0 b D^2 F_c (1 - \eta_0)\}^2 / h_0$, ($g_1 = 0.76$ in this test);
 $c\delta_y = \{(h_0^3 / 12 E_c I_e) + (1.2 h_0 / 0.43 E_c b D)\} cQ_y / \alpha y$, $\alpha y = (0.043 + 1.64 N P_t + 0.043 a/D + 0.33 \eta_0) (d/D)^2$ = stiffness deterioration factor at yielding, n = ratio of modulus of elasticity of reinforcing bar to that of concrete;
 $cQ_{BU} = \{0.8 \alpha t \sigma_y D + 0.5 \eta_0 b D^2 F_c (1 - \eta_0)\}^2 / h_0$;
 $cQ_{SU} = (0.9 + \sigma_0 / 250) \{0.23 k_u k_p (F_c + 180) / (h_0 / d + 0.23) + 2.7 \sqrt{P_w w_{oy}}\} b j$, $k_u = 0.9$ (in this test), $k_p = 0.82 P_t^{0.23}$, $P_t = a_t / b d$ (%), w_{oy} = yield stress for shear reinforcement of hoops.

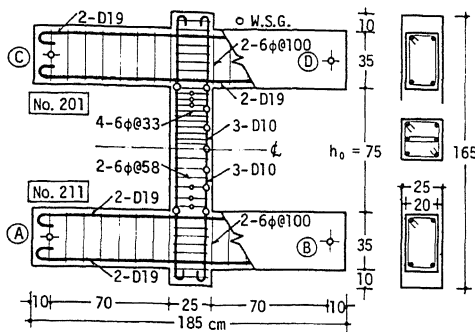


Fig.1 Details of Specimen

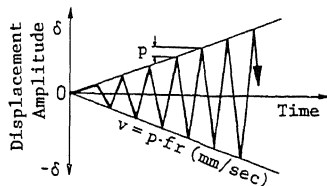
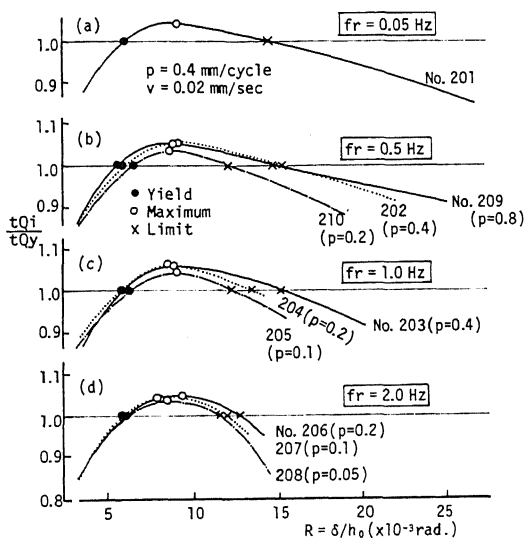


Fig.3 Loading Pattern



Series I: No. 201~210

Fig.5 Load-Deflection Envelope Curves

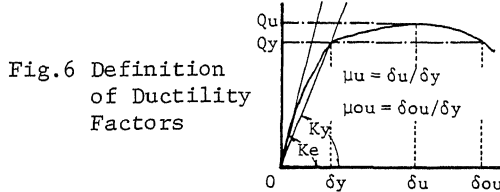


Fig.6 Definition of Ductility Factors

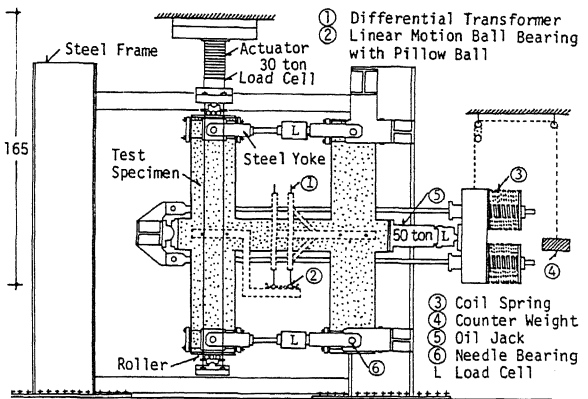


Fig.2 Test Setup

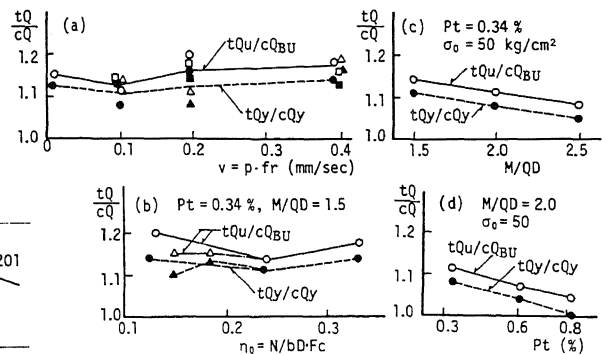


Fig.4 Comparisons of Measured Shear and Computed Value (tQ/cQ)

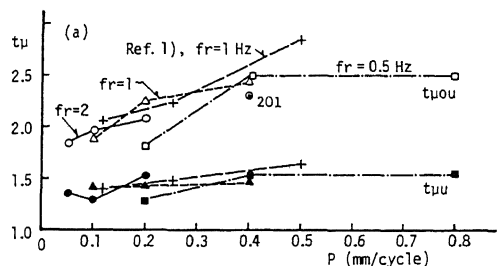


Fig.7(a) Relationship Between $tμ$ and p

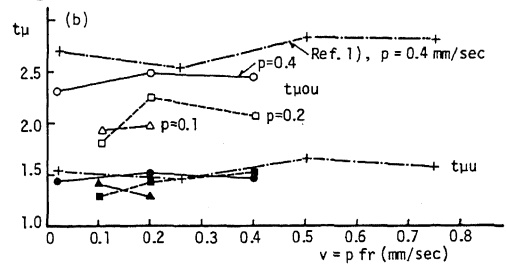


Fig.7(b) Relationship Between $tμ$ and v

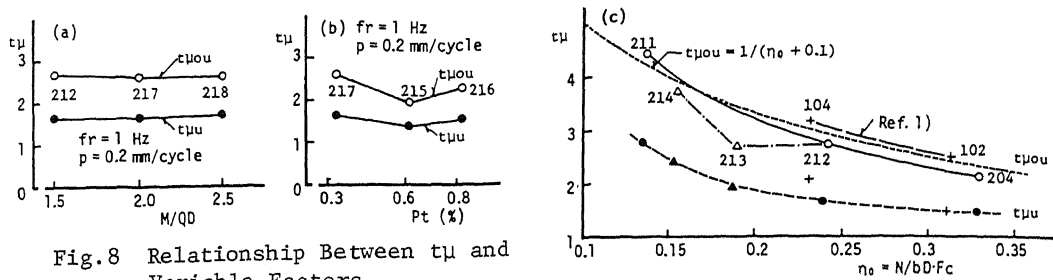


Fig.8 Relationship Between τ_{μ} and Variable Factors

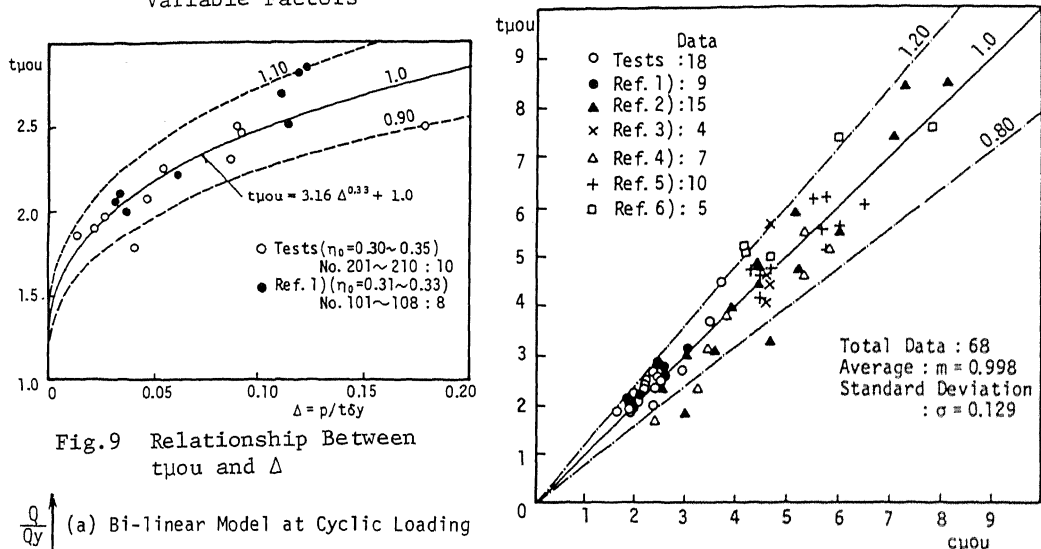


Fig.9 Relationship Between $\tau_{\mu ou}$ and Δ

Fig.10 Comparison of $\tau_{\mu ou}$ and $c_{\mu ou}$

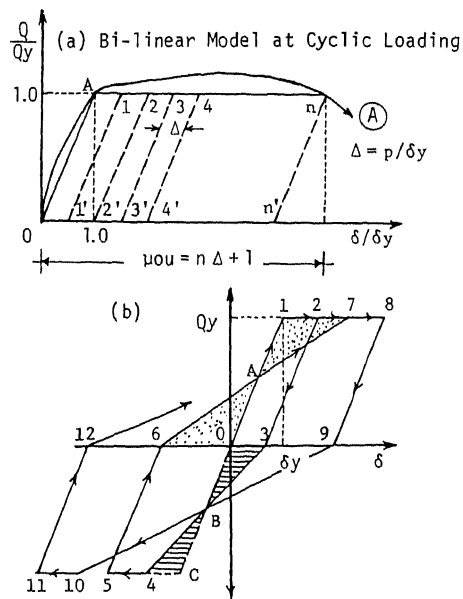


Fig.11 Imaginary Models

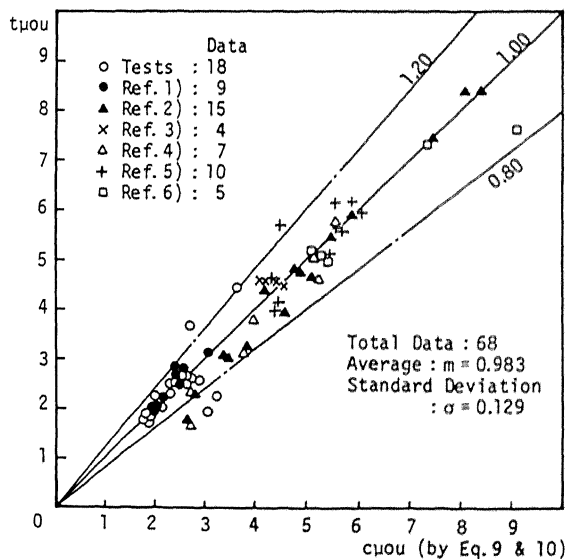


Fig.12 Comparison of $\tau_{\mu ou}$ and $c_{\mu ou}$